Hindawi Publishing Corporation
Active and Passive Electronic Components
Volume 2008, Article ID 134805, 8 pages
doi:10.1155/2008/134805

Research Article

A New Fractal-Based Design of Stacked Integrated Transformers

Goran Stojanović, Milan Radovanović, and Vasa Radonić

Faculty of Technical Sciences, University of Novi Sad, Trg Dositeja Obradovića 6, 21000 Novi Sad, Serbia

Correspondence should be addressed to Goran Stojanović, sgoran@uns.ns.ac.yu

Received 1 December 2007; Accepted 29 February 2008

Recommended by Tibor Berceli

Silicon-based radio-frequency integrated circuits are becoming more and more competitive in wide-band frequency range. An essential component of these ICs is on-chip (integrated) transformer. It is widely used in mobile communications, microwave integrated circuits, low-noise amplifiers, active mixers, and baluns. This paper deals with the design, simulation, and analysis of novel fractal configurations of the primary and secondary coils of the integrated transformers. Integrated stacked transformers, which use fractal curves (Hilbert, Peano, and von Koch) to form the primary and secondary windings, are presented. In this way, the occupied area on the chip is lower and a number of lithographic processes are decreased. The performances of the proposed integrated transformers are investigated with electromagnetic simulations up to 20 GHz. The influence of the order of fractal curves and the width of conductive lines on the inductance and quality factor is also described.

1. INTRODUCTION

Constant growth of wireless applications brought to an intensive need for mobile communications and mobile communication devices. Due to a growing need for wireless communication devices, radio frequency and wireless market is continuing its development. The integrated transformer is an essential component in many RF and microwave integrated circuits [1–8]. Although significant efforts have been made in order to improve the characteristics of integrated transformers [9–12], it is still a great problem to bring in piece the opposite demands for low cost, low supply voltage, and low power dissipation, but small occupied area and high frequency of operation in RF implementation of these transformers. Commonly used transformers are fabricated on lossy silicon substrate; hence they are from the start limited to a lower quality factor, coupling coefficient and high parasitic effects between the component and the substrate. Arbitrary transformer layouts also impact the transformer characteristics. Various transformers layouts including parallel winding, interwound winding, overlay winding, and concentric spiral winding were presented in [13]. Planar transformers generally have lower self-inductance, parasitic capacitances, and coupling factor, but higher resonant frequency comparing with the stacked transformers, which engage less chip area and have higher inductance values and lower quality factor [14]. The width of conductive lines (usually have the square spiral shape), spacing between coils, and material used for their fabrication also have influence on overlay characteristics of the transformer. However, papers that present other layout geometries (apart from square spiral) of the primary and secondary coils are very rare.

The unique property of fractal curves is that, after an infinite number of iterations, their length becomes infinite although the entire curve fits into the finite area. This space-filling property can be exploited for the miniaturization of the integrated transformers. Due to the technology limitations such as a minimal line width and spacing achievable by the fabrication process and because of its degree of complexity, the ideal fractal cannot be built. Our research is limited to prefractals with a low degree of iteration (or low order). In this work, we present novel layouts of the primary and secondary windings in the shape of fractal curves and demonstrate a comprehensive analysis of the shape and order fractal curves influence on the inductance and quality factor

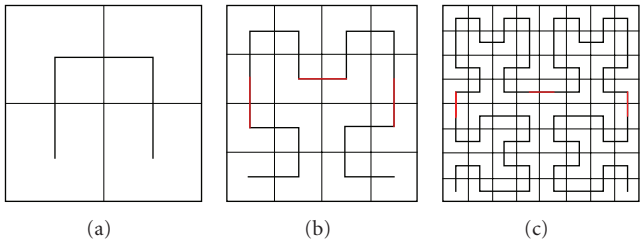

Figure 1: Hilbert curve (iteration 1, iteration 2, and iteration 3).

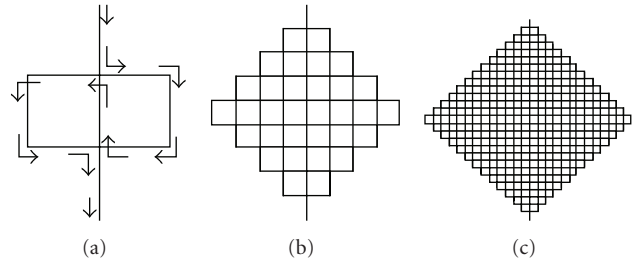

Figure 2: Peano curve (iteration 1, iteration 2, and iteration 3).

of the stacked transformers for RFICs applications. The simulation has been generated using the Microwave Office software package [15].

2. A BRIEF OVERVIEW OF USED FRACTAL CURVES

Fractals are a whole new set of geometrical objects featuring two main common properties: self-similarity and fractional dimension. There are many mathematical structures that are fractals; for example, Sierpinski's gasket, Peano curve, von Koch's snowflake, the Mandelbrot set, the Hilbert curve, and so forth [16–18]. In this paper, Hilbert curve, Peano curve, and von Koch curve have been used. The space-filling properties of these curves make them attractive candidates for use in the design of the primary and secondary windings of integrated fractal transformers.

Hilbert curve

Hilbert curves are built through an iterative procedure that generates almost self-similar structures. In addition, Hilbert curves are space-filling curves, meaning that in the limit the fractal curve fills the whole space. The capability to pack conductive lines in a small space following a Hilbert curve is very appealing for manufacturing windings of on-chip transformers. The first three steps in the construction of the Hilbert curve are shown in Figure 1.

Peano curve

The original Peano curve is a base-motiffractal that uses a line segment for the base and the motif depicted in Figure 2(a). To generate the Peano curve, it is necessary to start with a line segment and substitute it with the motif. After that, every one of the 9 line segments in the figure is taken and substituted with the motif again. At the end, a square is obtained as it is illustrated in Figure 2(c). In the motif, there are 9 identical line segments and the size of each is 1/3 of the original line segment.

Koch curve

Koch curve is a fractal curve characterized by such properties as a curve that is infinitely long, contained within a finite region, and not differentiable at any point (they just have corners). A geometric construction scheme for the Koch curve is shown in Figure 3.

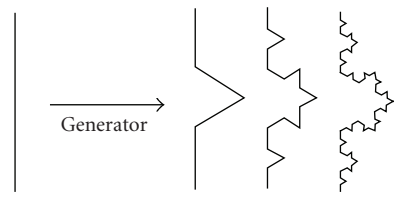

Figure 3: A geometrical construction of standard Koch curves.

3. DESIGN OF FRACTAL INTEGRATED TRANSFORMERS

Implementations and design of monolithic transformers consist of different trade-offs, which need to be considered in the geometry of the transformer layout. The inductance is determined by the primary or secondary windings (coils) lateral dimensions. Parasitic capacitances and resistances are determined by both lateral and vertical dimensions. Conventional configurations include interleaved and stacked transformer, with the spiral geometry of coils. These configurations offer varying trade-offs among self-inductance, mutual coupling coefficient, Q-factor, resonant frequency, and occupied area. For example, interleaved transformers (with square spiral shape) offer higher resonant frequency and medium coupling, whereas the stacked transformers offer high coupling and self-inductance but also high parasitic capacitances.

We have designed novel configurations of on-chip stacked transformers, where the primary and secondary windings have shapes of different fractal curves. Figure 4(a) depicts a schematic symbol and Figure 4(b) shows a stacked transformer model for simulation in the electromagnetic simulator Microwave Office. The main features of the transformers under study were assumed as follows. The silicon substrate was used with the thickness of 500 μm and the resistivity of 10 $\Omega\cdot$cm (Figure 4(c)). The thickness of metal layers for the primary and secondary coils is 1 μm. The oxide thickness between the silicon substrate and a metal layer for the secondary coil is 3 μm and between metal layers for the secondary (a lower layer) and the primary (an upper layer) coils is 1 μm. Aluminum is used as a conductive material with conductivity $\sigma = 3.53\cdot 10^7$ S/m. As the secondary winding is closer to the substrate, it is expected that its losses would be higher than those in the primary winding and therefore quality factor of the secondary coil would be lower than for primary coil. It is important to note

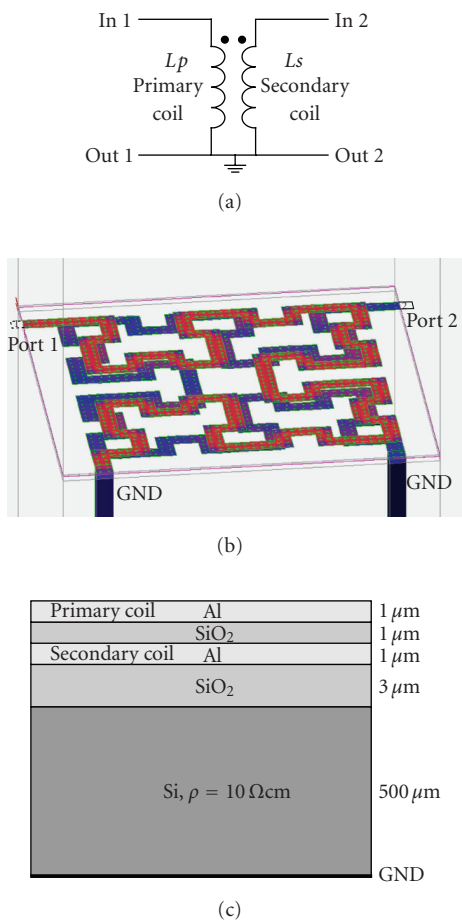

Figure 4: A stacked fractal transformer: (a) schematic symbol, (b) 3D model, and (c) the cross-section.

that the whole primary (and also secondary) coil occupies only one metal layer in contrast to all spiral realizations, which required more metal layers for underpass or overpass.

A stacked transformer depicted in Figure 4(b), where the primary and secondary coils have the shape of 3rd-order Hilbert curve, has turn ratio 1 : 1. Port 1 and port 2 are input ports for the primary and secondary coils, respectively, whereas the other terminals are grounded.

The losses in the conductive segments are taken into account through two parameters, which are presented in Figure 5. The low frequency parameter (Rdc) specifies the DC resistance of the planar conductor (in ohms/square). The DC resistance is the resistance of the conductor assuming a uniform current distribution in the cross-section of the conductor. The high frequency loss coefficient (Rhf) specifies the loss associated with the conductor at frequencies, where the thickness of the conductor is significantly thicker than the skin depth. Since the loss associated with the skin depth effects are proportional to the square root of frequency, the skin depth loss coefficient is multiplied by the square root of frequency to provide an ohms/square value that is used for loss computations. At low frequencies, the DC resistance is used in the computation of conductor loss, while at high frequencies the high frequency loss coefficient

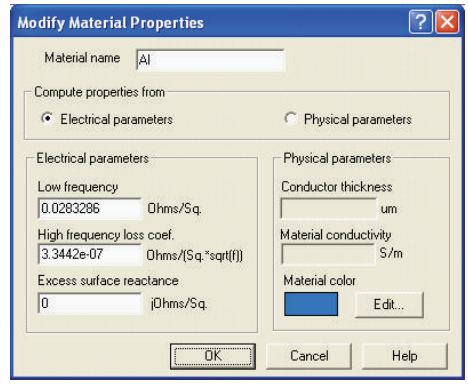

Figure 5: The electrical parameters of conductive material (Al) including high frequency loss coefficient.

is used to compute conductor loss. In the transition region (frequencies where the skin depth is close to the thickness of the conductor) both factors are used. In this paper, typical values of these parameters have been Rdc = 0.02832 and Rhf = $3.34 \cdot 10^{-7}$, according to the metal thickness and conductivity, for the aluminum conductive layer.

4. RESULTS AND DISCUSSION

The layout topology of the windings of the integrated transformers strongly depends on the application of the transformer. In this paper, the stacked configuration of monolithic transformer is analyzed. Stacked transformer, or vertical coupling structure, represents a multiple conductor layer structure. This configuration has the advantage of area efficiency and higher mutual coupling between the windings due to placing the primary coil on top of the secondary. Stacked transformers mainly have high coupling factor (k-factor), up to 0.9, and high mutual inductance. The primary and the secondary windings are placed in adjacent metal layers causing different distances from the substrate. In order to improve its characteristics, the windings are placed in slightly offset position (horizontally or diagonally shifted), resulting in lower parasitic capacitance and consequently higher Q-factor and resonant frequency.

4.1. *Transformer windings in the form of Hilbert curves*

In this subsection, we investigate behavior of transformer parameters with variations of the Hilbert curves iteration and the width of conductive segments of the primary and secondary parts of the transformer.

In the first example, the primary and secondary windings are made in the form of Hilbert curve of the third order ($N = 3$). The width of the conductive lines for the primary and secondary windings (w_p and w_s) are 10 μm and after that 6 μm at overall occupied area 336 μm $\times$336 μm. Figure 6 shows a 3D view of these transformers. The performances of the proposed transformers were determined using EMSight, the EM simulator in Microwave Office. Figure 7 illustrates

Table 1: The performance comparison of different transformer realizations.

Ref.	Configuration	Lp [nH]	Qp	SRF [GHz]
[11]	Differential square spiral transformer	0.8	5.2 peak @ 5 GHz	10
[12]	Interleaved 3 turn square spiral transformer	5.32	5.77 peak @ 2.95 GHz	6.2
[13]	Interleaved square spiral transformer	8.5	NA	4.9
[14]	Differential square spiral transformer	5.5	10 peak @ 1.7 GHz	NA
This work	Stacked transformer, Hilbert $N = 3$, $w = 10\,\mu$m	0.6	5.95 peak @ 8.4 GHz	18.8

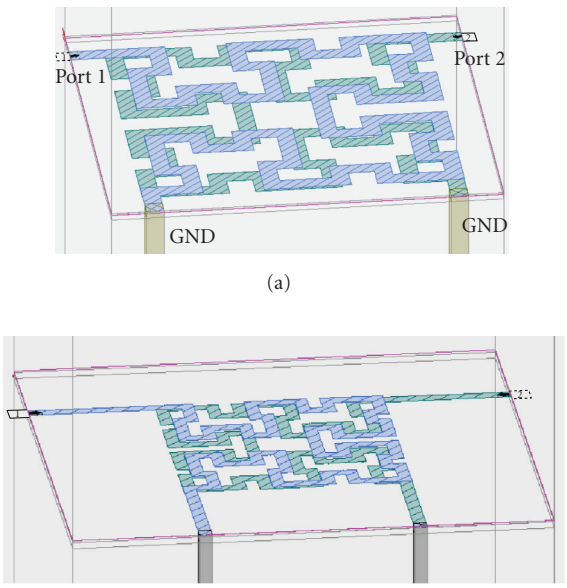

Figure 6: A monolithic stacked transformer realized with two 3rd-order Hilbert curve, (a) $w_p = w_s = 10\,\mu$m, (b) $w_p = w_s = 6\,\mu$m.

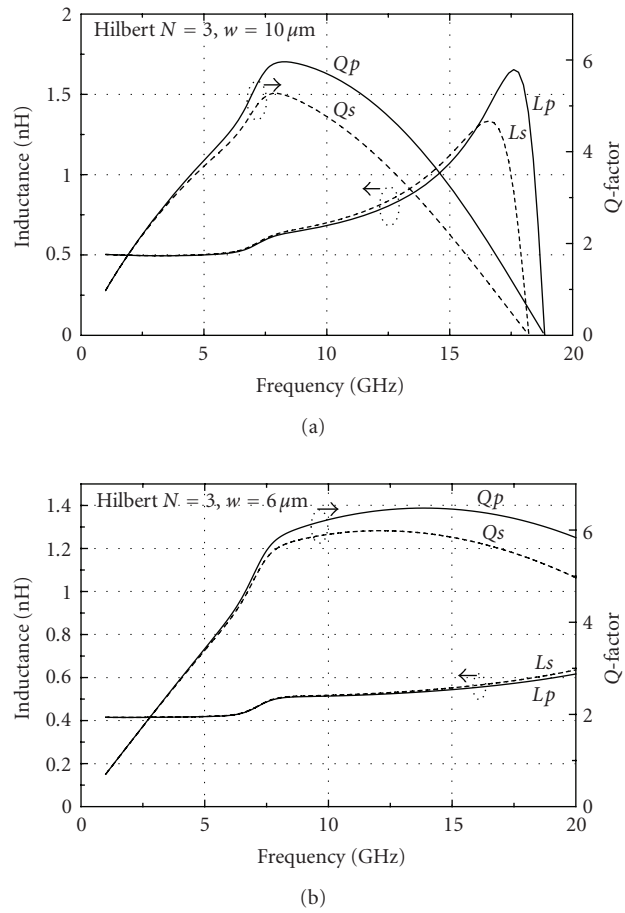

Figure 7: The inductance and quality factor as a function of frequency for stacked transformer, (a) 3rd-order Hilbert curve, $w_p = w_s = 10\,\mu$m, (b) 3rd-order Hilbert curve, $w_p = w_s = 6\,\mu$m.

the inductance and Q-factor of transformer structures as a function of frequency.

From Figure 7 it can be seen that the inductances of the primary and secondary coils are approximately the same (ratio 1 : 1) in the wide frequency range. For the same order of fractal curves, greater values of the quality factor can be obtained for a smaller width of the metal trace. Figure 7 shows that a wider metal strip has a lower peak Q and resonant frequency, although it has a higher Q at low frequencies. This can be explained by the fact that wider metal traces lead to larger parasitic capacitances between coils and substrate, and consequently lower Q-factor and self-resonant frequency.

In the next simulation the order of fractal curve is increased. The primary and secondary winding are realized using 4th-order of Hilbert curve ($N = 4$) as can be seen in Figure 8. Technological parameters were the same as in the previous example.

The simulation results for the inductance and quality factor as a function of frequency are depicted in Figure 9, for the widths of metal strip of $10\,\mu$m and $6\,\mu$m, respectively. It can be seen that the stacked Hilbert transformer with fractal curves of the 4th order achieves only the inductance improvement (due to longer total conductive lines), but Q-factor and self-resonant frequency are smaller comparing to the 3rd-order curves with the same widths of the primary and secondary coils.

The proposed Hilbert transformer with $w = 6\,\mu$m exhibited a simulated Lp around 1.3 nH at 3 GHz, which is approximately 25% lower than that of a Hilbert structure with $w = 10\,\mu$m. However, the transformer with $w = 6\,\mu$m has higher values of the quality factor. This means that higher

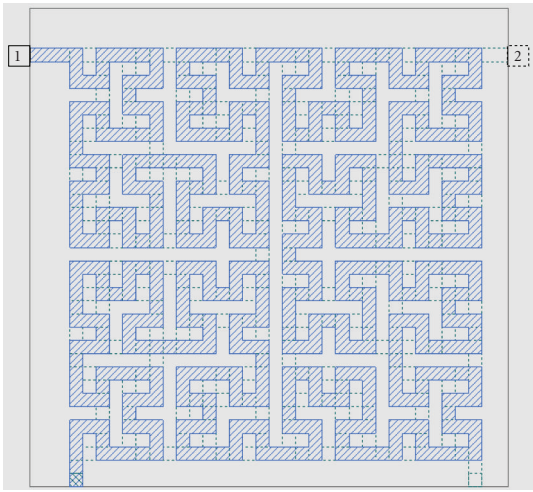

(a)

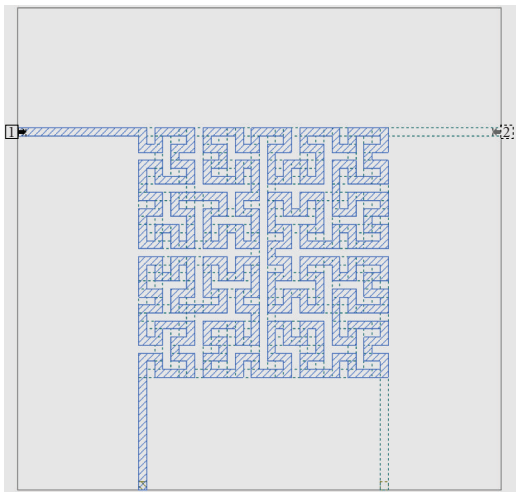

(b)

Figure 8: A top view of fractal transformers realized with two Hilbert curves $N = 4$, (a) $w_p = w_s = 10\,\mu$m, (b) $w_p = w_s = 6\,\mu$m.

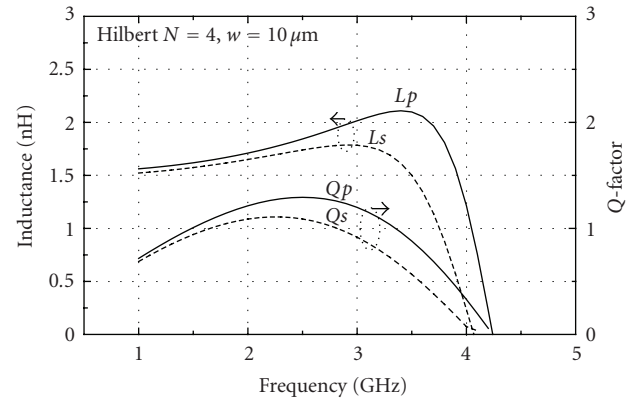

(a)

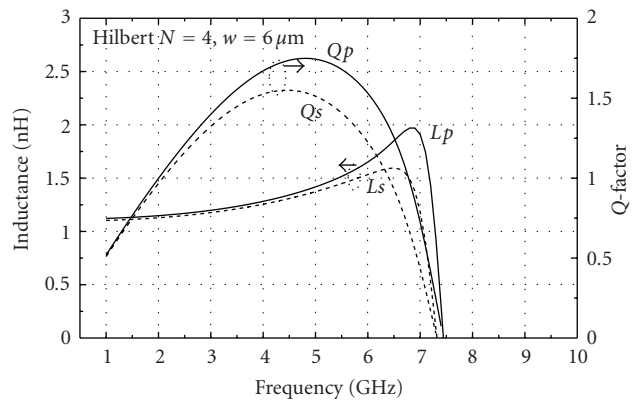

(b)

Figure 9: Frequency characteristics of the inductance and quality factor of integrated stacked transformer realized with 4th order of Hilbert curve (a) $w_p = w_s = 10\,\mu$m, (b) $w_p = w_s = 6\,\mu$m.

Q value of a Hilbert transformer structures is mainly due to lower series resistance (and parasitic capacitance).

To conclude this subsection, it is important to point out that a good Qp around 6, and Qs around 5.3 (Figure 7(a)) were achieved at 8.4 GHz, respectively. This is better than results for differential or interleaved transformer with square spiral in open literature [11, 12]. Note that there is, also, a significant increase in the self-resonant frequency (*SRF*). The simulation results show that using Hilbert fractal layouts for the primary and secondary windings of stacked transformers, similar or better performances can be achieved comparing to the published results for monolithic transformers, as listed in Table 1.

This improving performance is evident regarding increasing *SRF* and Q-factor, whereas the inductance values are reasonably smaller due to higher value of the negative mutual inductance between segments of a conductive strip with the shape of Hilbert fractal curve.

4.2. The primary and secondary windings in the form of von Koch curves

In this subsection, the Koch fractal curves of the third and forth order are used for realization of the primary and secondary windings of the stacked transformers. The geometrical and technological parameters are the same as in the earlier simulations. In the first realization, the primary and secondary coils are designed of three serially connected 3rd-order Koch curves with the width of conductive (aluminum) lines $w_p = w_s = 10\,\mu m$ and after that $w_p = w_s = 6\,\mu$m. To compare results for this fractal curves and Hilbert ones, the overall area is the same as in the previous cases. The 3D and the top view of the primary and secondary windings are depicted in Figure 10, for $w_p = w_s = 10\,\mu$m. In order to minimize the parasitic capacitance between the primary and the secondary coils of transformers, the secondary coil is rotated with the respect to the primary ones for an angle of 90 degrees.

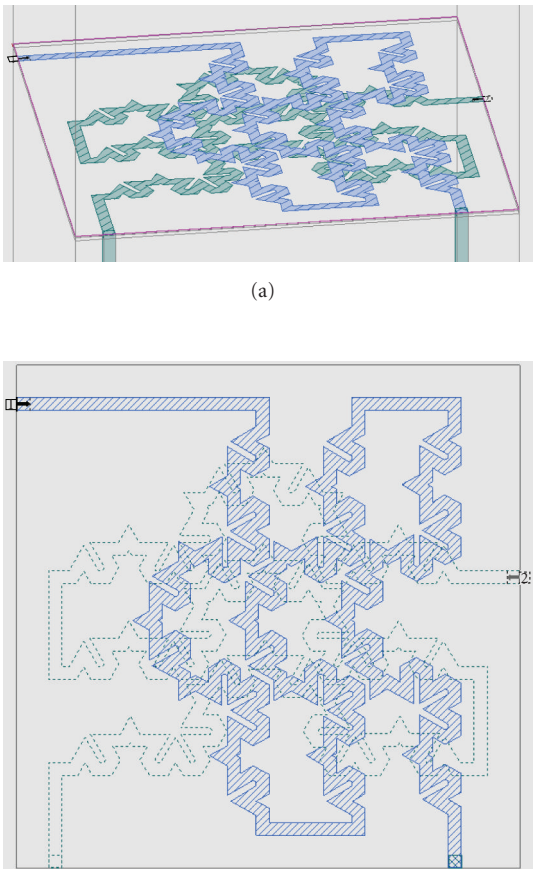

(a)

(b)

Figure 10: A Koch fractal transformer, (a) 3D view (b) the top view.

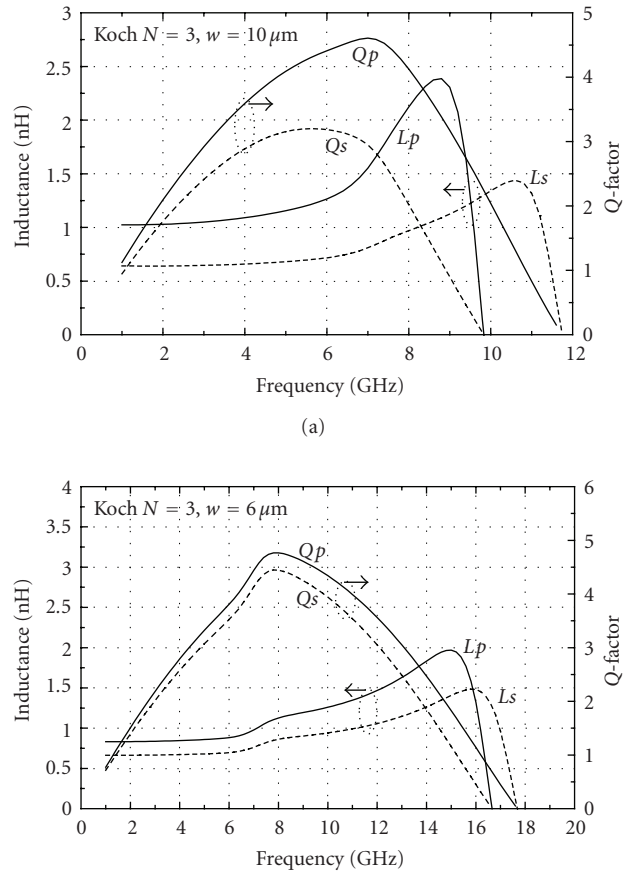

(a)

(b)

Figure 11: Dependence of Q-factor and inductance as a function of frequency for transformer with (a) $w_p = w_s = 10\,\mu$m, (b) $w_p = w_s = 6\,\mu$m.

In Figure 11, dependence of the primary and secondary inductances and corresponding quality factors are shown as a function of frequency for $w_p = w_s = 10\,\mu$m (Figure 11(a)) and for $w_p = w_s = 6\,\mu$m (Figure 11(b)).

Although the primary and the secondary are designed to have the same shape and the width of conductive lines, obtained values of their inductance and corresponding values of quality factor are slightly different due to the existence of the back-side metallization. The current induced in the metallization layer lowers the inductance values in both transformer structures, since it flows in the opposite direction than the current in windings. The inductance of the secondary winding is more affected because it is placed closer to the metallization. It can be observed that with an increase of frequency, Q-factor grows initially and reaches its maximal value. At higher frequencies, substrate losses and the ac resistance of conductive lines increases faster than the inductive reactance, which results in a decrease of the quality factor appears. The higher self-resonant frequency is obtained for the transformer with the smaller line width due to the low parasitic capacitances between windings and metallization plane and therefore this structure can be used in the widest frequency range.

4.3. The primary and secondary windings in the form of Peano curves

The Peano fractal curves of the second order are also used for realization of the primary and secondary coils of integrated stacked transformer. The layout of the transformer is shown in Figure 12 (3D view in Figure 12(a) and the top view in Figure 12(b)) with $w_p = w_s = 6\,\mu$m. As can be seen, the primary and secondary winding are slightly shifted with the aim of the minimization of the parasitic capacitance between the coils.

The simulation results for the inductance and quality factor are presented in Figures 13(a) and 13(b). Figure 13(a) shows the obtained values of Q-factors for the primary coil (Qp) and the secondary coil (Qs), and for corresponding inductances with $w_p = w_s = 10\,\mu$m, whereas Figure 13(b) shows these results for the structure with $w_p = w_s = 6\,\mu$m. In this case, better values of the quality factor were obtained for the structure with $w_p = w_s = 10\,\mu$m ($Qp = 4.7$, and $Qs = 3.4$ at 7.5 GHz). The higher Qp and Qs for this structure are attributed to a larger distance between neighboring segments (greater step) that means lower overall capacitance between the primary (and secondary) coil and the silicon substrate.

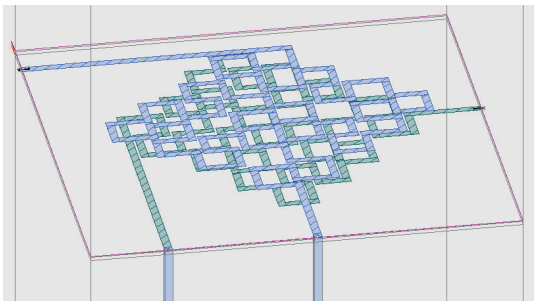

(a)

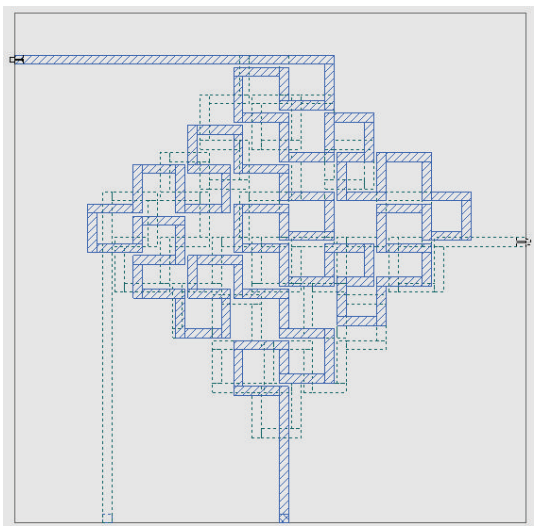

(b)

Figure 12: The Peano ($N = 2$) fractal transformer: (a) 3D view, (b) the top view.

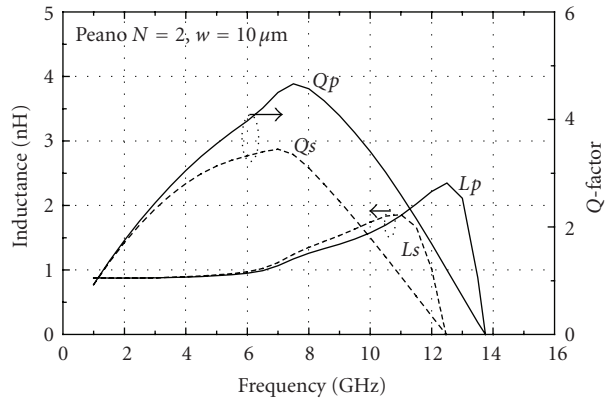

(a)

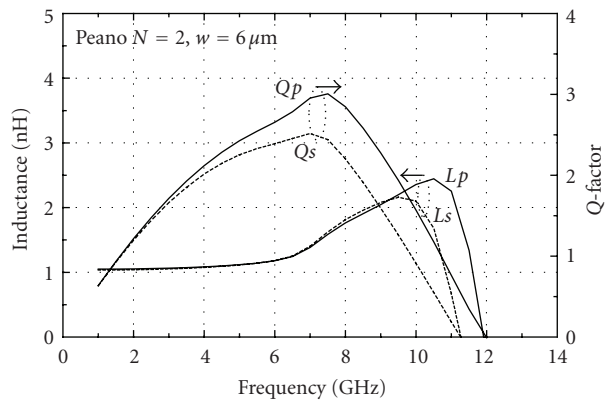

(b)

Figure 13: Q-factor and inductance versus frequency for Peano transformer with (a) $w_p = w_s = 10\,\mu$m, (b) $w_p = w_s = 6\,\mu$m.

Comparing proposed integrated transformers it can be concluded that the configuration with 3rd-order Hilbert curve has a maximal value of the Q-factor and self-resonant frequency, afterwards realizations with Koch and Peano curves. The minimal Q-factor has the stacked transformer with 4th-order Hilbert curve thanks to the largest occupied area and as a result the biggest parasitic capacitance value. As can be seen from Figure 7(b), the best Qp around 6.8, and Qs around 5.9 were achieved at approximately 12 GHz. It is important to emphasize that by comparison with published results there is also a significant increase in self-resonant frequency in the presented transformer structures.

5. CONCLUSION

The integrated transformer characteristics and performances greatly depend on geometrical and process parameters. In this paper, the novel fractal stacked transformers were analyzed using full-wave EM simulations and compared in terms of the inductance and quality factor. Simulation results show that using fractal layouts for the primary and secondary windings, similar or better performances can be achieved in comparison with earlier published results for monolithic transformers with square spiral geometry. The presented results mean that transformer configurations with fractal curves can be very useful for RF-IC designers to design high-performance RF and microwave integrated circuits.

REFERENCES

[1] Y. K. Koutsoyannopoulos and Y. Papananos, "Systematic analysis and modeling of integrated inductors and transformers in RF IC design," *IEEE Transactions on Circuits and Systems II*, vol. 47, no. 8, pp. 699–713, 2000.

[2] Y.-S. Choi, J.-B. Yoon, B.-I. Kim, and E. Yoon, "A high-performance MEMS transformer for silicon RF ICs," in *Proceedings of the 15th IEEE International Conference on Micro Electro Mechanical Systems (MEMS '02)*, pp. 653–656, Las Vegas, Nev, USA, January 2002.

[3] J. Y. Park and J. U. Bu, "Packaging compatible microtransformers on a silicon substrate," *IEEE Transactions on Advanced Packaging*, vol. 26, no. 2, pp. 160–164, 2003.

[4] J. Y. Park, Y. J. Chang, and J. U. Bu, "Monolithically integrated 3D micro-inductors and micro-transformers for RF applications," in *Proceedings of the 8th International Symposium on Advanced Packaging Materials (ISAPM '02)*, pp. 362–363, Stone Mountain, Ga, USA, March 2002.

[5] Y. J. Yoon, Y. Lu, R. C. Frye, and P. R. Smith, "Modeling of monolithic RF spiral transmission-line balun," *IEEE Transactions on Microwave Theory and Techniques*, vol. 49, no. 2, pp. 393–395, 2001.

[6] H. Y. D. Yang and J. A. Castaneda, "Design and analysis of on-chip symmetric parallel-plate coupled-line balun for silicon RF integrated circuits," in *Proceedings of IEEE Radio Frequency Integrated Circuits Symposium (RFIC '03)*, pp. 527–530, Philadelphia, Pa, USA, June 2003.

[7] A. M. Niknejad and R. G. Meyer, "Analysis, design, and optimization of spiral inductors and transformers for Si RF ICs," *IEEE Journal of Solid-State Circuits*, vol. 33, no. 10, pp. 1470–1481, 1998.

[8] A. H. Aly and B. Elsharawy, "Modeling and measurements of novel high k monolithic transformers," in *Proceedings of IEEE MTT-S International Microwave Symposium*, vol. 2, pp. 1247–1250, Philadelphia, Pa, USA, June 2003.

[9] A. Zolfaghari, A. Chan, and B. Razavi, "Stacked inductors and transformers in CMOS technology," *IEEE Journal of Solid-State Circuits*, vol. 36, no. 4, pp. 620–628, 2001.

[10] K. T. Ng, B. Rejaei, and J. N. Burghartz, "Substrate effects in monolithic RF transformers on silicon," *IEEE Transactions on Microwave Theory and Techniques*, vol. 50, no. 1, pp. 377–383, 2002.

[11] O. El Gharniti, E. Kerhervé, J.-B. Bégueret, and P. Jarry, "Modeling of integrated monolithic transformers for silicon RF IC," in *Proceedings of the 11th IEEE International Conference on Electronics, Circuits and Systems (ICECS '04)*, pp. 137–140, Tel Aviv, Israel, December 2004.

[12] J. Jaehning, D. R. Allee, E.-B. El-Sharawy, T. L. Alford, N. Yazdi, and D. J. Allstot, "Monolithic transformers in a five metal CMOS process," in *Proceedings of IEEE International Symposium on Circuits and Systems (ISCAS '02)*, vol. 2, pp. 807–810, Phoenix, Ariz, USA, May 2002.

[13] J. R. Long, "Monolithic transformers for silicon RF IC design," *IEEE Journal of Solid-State Circuits*, vol. 35, no. 9, pp. 1368–1382, 2000.

[14] M. Straayer, J. Cabanillas, and G. M. Rebeiz, "A low-noise transformer-based 1.7 GHz CMOS VCO," in *Proceedings of IEEE International Solid-State Circuits Conference (ISSCC '02)*, vol. 1, pp. 286–287, San Francisco, Calif, USA, Fedbruary 2002.

[15] Microwave Office 2001, Applied Wave Research, Inc.

[16] H. O. Peitgen, H. Jürgens, and D. Saupe, *Chaos and Fractals: New Frontiers of Science*, Springer, New York, NY, USA, 1992.

[17] P. Emp, S. Joan, and S. C. del Vallès, *Fractal Miniaturization in RF and Microwave Networks*, Fractus, Barcelona, Spain, 2001.

[18] Fractalcoms final report, Project no. IST-2001-33055, http://www.tsc.upc.es/fractalcoms/.